

Motion and pinning of discrete interfaces

A. Braides^{*} M.S. Gelli[†] M. Novaga[‡]

Abstract

We describe the motion of interfaces in a discrete environment by coupling the minimizing movements approach by Almgren, Taylor and Wang and a discrete-to-continuous analysis. We show that below a critical ratio of the time and space scalings we have no motion of interfaces (pinning), while above that ratio the discrete motion is approximately described by the crystalline motion by curvature on the continuum described by Almgren and Taylor. The critical regime is much richer, exhibiting a pinning threshold (small sets move, large sets are pinned), partial pinning (portions of interfaces may not move), pinning after an initial motion, “quantization” of the interface velocity, and non-uniqueness effects.

1 Introduction

A wide class of lattices energies; *i.e.*, depending on a discrete variable $u = \{u_i\}$ indexed by the nodes i of a lattice, can be interpreted as interfacial energies. The simplest of such energies are functionals defined on binary systems, where u_i may only take two values, *e.g.* the values $+1$ and -1 (*spin systems*). Their prototype is

$$P(u) = \sum_{\text{n.n.}} (u_i - u_j)^2, \quad (1.1)$$

where the sum runs over all *nearest neighbors* (n.n.) in \mathbb{Z}^n ; *i.e.*, all pairs of indices i and j in the n -dimensional cubic lattice \mathbb{Z}^n such that $|i - j| = 1$. Note that thanks to the condition $u_i^2 = u_j^2 = 1$ the energy density of P only differs by an additive constant from the usual *ferromagnetic* energy density $-u_i u_j$ for Ising systems. After identifying a function u with the set E obtained as the union of all (closed) unit cubes with centers i such that $u_i = 1$, we see that P can be rewritten as a perimeter functional

$$P(E) = 4 \mathcal{H}^{n-1}(\partial E).$$

In the framework of the analysis of lattice systems by a continuous variational approximation (see [1, 2, 3, 4, 12, 10]) and in view of their connections to physical phenomena linked to phase separation and motion of dislocations (see

^{*}Dipartimento di Matematica, Università di Roma “Tor Vergata”, via della Ricerca Scientifica, 00133 Roma, Italy, email: braides@mat.uniroma2.it

[†]Dipartimento di Matematica, Università di Pisa, largo Pontecorvo 5, 56216 Pisa, Italy, email: gelli@dm.unipi.it

[‡]Dipartimento di Matematica, Università di Pisa, largo Pontecorvo 5, 56216 Pisa, Italy, email: novaga@dm.unipi.it

e.g. [7, 14, 16, 19, 21, 23]), we are interested in energy-driven motions deriving from this type of functionals. From a different standpoint, since such perimeter energies arise in the study of the motion by mean curvature (see [6, 13, 17]), the same question can be interpreted as the analysis of discreteness effects on such motions, with obvious implication for their numerical study. A third motivation derives from the study of geometric motions in inhomogeneous environments (see, e.g., [9, 20, 15, 18]), of which the discrete one may be considered as a simpler version. Finally, such motions can be compared with others where the interplay between time and space discretization is crucial (as in [8]).

Since no motion by ‘gradient flow’ is directly possible in the discrete environment (as all u are isolated points), we perform an analysis in a discrete-to-continuous framework, where we scale the lattice and the energy P by introducing a small parameter ε . As a result, we have the energies

$$P^\varepsilon(u) = \frac{1}{4}\varepsilon^{n-1} \sum_{\text{n.n.}} (u_i - u_j)^2,$$

where now $u : \varepsilon\mathbb{Z}^n \rightarrow \{\pm 1\}$. This functional may again be identified with the perimeter

$$P^\varepsilon(E) = \mathcal{H}^{n-1}(\partial E),$$

with the constraint that E be the union of cubes of side length ε . These energies Γ -converge, as $\varepsilon \rightarrow 0$, to an *anisotropic (crystalline) perimeter functional*

$$\mathcal{F}(E) = \int_{\partial E} \|\nu\|_1 d\mathcal{H}^{n-1},$$

where $\|\nu\|_1 = \sum_{k=1}^n |\nu_k|$ is the l^1 -norm of the unit normal ν to ∂E (see [1]). Note that the geometric constraint on E is lost in the limit and the domain of \mathcal{F} are all sets of finite perimeter in \mathbb{R}^n . On the other hand, the anisotropies of the square lattice reappear in a relaxed form through the anisotropy of the l^1 -norm.

A study of the motion driven by the curvature related to the crystalline perimeter \mathcal{F} in the continuous framework has been performed by Almgren and Taylor in 2D. Their approach follows the one proposed by Almgren, Taylor and Wang [6] to deal with mean curvature flow, by first introducing a time step $\tau = \Delta t$ and constructing a ‘discrete motion’ E_τ^i from an initial datum E^0 by successive minimizations

$$E_\tau^0 = E^0, \quad E_\tau^{i+1} \in \operatorname{argmin} \left\{ \mathcal{F}(A) + \frac{1}{\tau} D(E, E_\tau^i) \right\},$$

where $D(E, F)$ is a suitably defined ‘distance’ between E and F . The passage to a continuous motion is then performed by defining $E_\tau(t) = E_\tau^{\lfloor t/\tau \rfloor}$ ($\lfloor s \rfloor$ denoting the integer part of s) and then letting $\tau \rightarrow 0$. A crucial step in this process is the definition of D as

$$D(E, F) = \int_{E \Delta F} \operatorname{dist}(x, \partial F) dx,$$

which in a way penalizes large variations of $x \mapsto \operatorname{dist}(x, \partial E_\tau^i)$ for $x \in \partial E_\tau^{i+1}$, thus providing some necessary symmetry of the motion. The limit motion by

crystalline curvature has been characterized in the two-dimensional case [5], showing in particular that self-similar motions are all obtained when the initial datum E^0 is a rectangle [22]. In this case the rectangles shrink to their common centre in finite time, the length of their sides $L_1(t)$ and $L_2(t)$ following the system of ODE's

$$\dot{L}_1 = -\frac{4}{L_2}, \quad \dot{L}_2 = -\frac{4}{L_1}.$$

Scope of our work is to show that we may perform a similar process, coupled with the passage from-discrete-to-continuous, for our discrete energies P^ε in the place of \mathcal{F} , that the resulting continuous motion can be compared with crystalline motion, but with additional features deriving from the discrete nature of the underlying energies. It must be remarked that it is not at all *a priori* clear that the continuous crystalline motion be related to the discrete one. In fact, if one repeats the piecewise-discretization reasoning as above for fixed ε , it is easily seen that the process stops after the first step, the motion is trivial $E_\tau(t) \equiv E_\varepsilon^0$ for $t > \tau$ (where E_ε^0 is an approximation of the initial datum in the domain of P^ε) and in the limit there is no motion for all (sufficiently regular) initial datum E^0 (*pinning*). By the Γ -limit analysis above, conversely, crystalline motion can be obtained by letting first $\varepsilon \rightarrow 0$ and then $\tau \rightarrow 0$. The 'critical' motion will be obtained by letting both ε and τ tend to zero at the same time. The piecewise-minimization process can be repeated after choosing $\varepsilon = \varepsilon(\tau)$, and defining

$$E_\tau^0 = E^0, \quad E_\tau^{i+1} \in \operatorname{argmin} \left\{ P^\varepsilon(E) + \frac{1}{\tau} D_\varepsilon(E, E_\tau^i) \right\},$$

(see the precise formulation in Section 2) and a continuous limit $E(t)$ is then obtained as above by letting $\tau \rightarrow 0$ (Theorem 3.1).

With the choice of D_ε analogous to D above, we show that E coincides with crystalline mean curvature motion only when $\varepsilon \ll \tau$, while pinning for all initial data is obtained when $\tau \ll \varepsilon$. In general the limit motion depends on the ratio $\alpha = \tau/\varepsilon$, which we may assume fixed and not zero. The differences with the crystalline case can be highlighted by describing some features of the motion starting from an initial rectangle R^0 with sides of length L_1^0, L_2^0 (see Theorem 3.2):

- 1) (*pinning for large initial data*) if $L_1^0 > 2\alpha$ and $L_2^0 > 2\alpha$ then $E(t) \equiv R^0$;
- 2) (*quantized velocities*) if $L_1^0 < 2\alpha$ and $L_2^0 < 2\alpha$ then $E(t)$ is a rectangle with sides of length $L_1(t), L_2(t)$ following the system of ODE's

$$\dot{L}_1 = -\frac{2}{\alpha} \left\lfloor \frac{2\alpha}{L_2} \right\rfloor, \quad \dot{L}_2 = -\frac{2}{\alpha} \left\lfloor \frac{2\alpha}{L_1} \right\rfloor.$$

Note that the motion is uniquely defined even though the right-hand sides of the equations are discontinuous, and that the rectangles $E(t)$ are not all homothetic, even though they shrink to the centre of R^0 ;

- 3) (*partial pinning*) if $L_1^0 > 2\alpha$ and $L_2^0 < 2\alpha$, then only the shorter side moves with constant inward velocity $v_2 = \frac{1}{\alpha} \lfloor 2\alpha/L_2^0 \rfloor$ until $L_1(t) = 2\alpha$. Note in particular that this implies that only a *weak comparison principle* holds: if two initial data satisfy $E_1^0 \subset E_2^0$ the corresponding $E_i(t)$ do satisfy $E_1(t) \subseteq E_2(t)$, but $E_1^0 \neq E_2^0$ does not imply that $E_1(t) \subset\subset E_2(t)$ for $t > 0$;

- 4) (*non-uniqueness*) in the cases not covered above we may have non-uniqueness of the motion. Note that this happens even when the initial datum is a square

with sides of length $L^0 = 2\alpha$, which may stay pinned until an arbitrary time T after which it follows the unique motion given by (2); *i.e.*, with $\dot{L} = -\frac{2}{\alpha} \lfloor 2\alpha/L \rfloor$.

The phenomena described above are a consequence of the discrete nature of the functionals P^ε or, equivalently, of the constraint that the sets E_τ^i be the union of cubes of side length $\varepsilon(\tau)$. In this way, given that R^0 may be thought to be itself such a set and all minimal E_τ^i are rectangles, the absence of pinning is possible only when it is convenient to ‘shrink’ a side of R^0 at least by ε . Plugging the corresponding test set in the minimization problem above we obtain the condition $L_i^0 < 2\alpha$. The same discretization argument shows that indeed the rectangle sides must shrink exactly of a multiple of ε ; this can be shown to imply both the discreteness of the velocity, and the non-uniqueness phenomena corresponding to the case when we have a choice between two multiples of ε by which the side decreases.

Additional interesting phenomena arise in the analysis of the motion of more general initial data. A simple illustration is obtained by taking convex bounded (and for simplicity, smooth) initial data. In this case the four points with vertical or horizontal tangent have ‘infinite curvature’, while all other points are ‘locally pinned’. As a result, we have the immediate nucleation in $E(t)$ of four segments parallel to the coordinate axes with length L_i , which move with inward velocity $v_i = \frac{1}{\alpha} \lfloor 2\alpha/L_i \rfloor$ and satisfy the constraint that their endpoints lie on the boundary of the initial datum, until their length exceeds 2α or until two such segments meet (after which the description is a little more complex). Note that in particular this shows that we may have

5) *pinning of sets after an initial motion*

(see Examples 3.17 and 3.22). Moreover, the final pinned state may not be a square or a rectangle. This analysis actually carries over to sets which are not convex, and in particular shows the possibility of

6) *non-convex pinned sets*

(see Example 3.12).

2 Formulation of the problem

In the following we will be concerned with discrete parameters both in space and time. Following the pioneering approach of Almgren and Taylor for crystalline energies [5] we want to investigate the limiting behaviour of the flat motions associated with interfaces in a discrete lattice, letting both parameters tend to 0 at the same time.

2.0.1 Notation

If A is a Lebesgue-measurable set we denote by $|A|$ its two-dimensional Lebesgue measure. The symmetric difference of A and B is denoted $A\Delta B$, their Hausdorff distance by $d_{\mathcal{H}}(A, B)$.

If E is a set of finite perimeter then ∂^*E is its reduced boundary. The inner normal to E at a point x in ∂^*E is denoted by $\nu = \nu_E(x)$ (see, *e.g.*, [11]).

2.1 Perimeter energies on discrete sets

We will treat functionals with underlying lattices $\varepsilon\mathbb{Z}^2$ with vanishing grid size ε . For a set of indices $\mathcal{I} \subset \varepsilon\mathbb{Z}^2$ we will consider the energy

$$P^\varepsilon(\mathcal{I}) = \varepsilon \# \left\{ (\underline{i}, \underline{j}) \in \varepsilon\mathbb{Z}^2 : \underline{i} \in \mathcal{I}, \underline{j} \notin \mathcal{I}, |\underline{i} - \underline{j}| = \varepsilon \right\}. \quad (2.1)$$

As customary, in order to pass from discrete systems to a continuous formulation, it is convenient to identify sets of indices $\mathcal{I} \subset \varepsilon\mathbb{Z}^2$ with subsets of \mathbb{R}^2 (namely, union of cubes), and discrete energies with corresponding continuous ones. To this end we introduce some notation for the discrete spatial setting.

We denote by $Q = [-1/2, 1/2]^2$ the unit closed coordinate square of centre 0. With fixed space mesh $\varepsilon > 0$ and $\underline{i} \in \varepsilon\mathbb{Z}^2$, we denote by $Q_\varepsilon(\underline{i}) = \underline{i} + \varepsilon Q$ the closed coordinate square with side length ε centered in \underline{i} . To a set of indices $\mathcal{I} \subset \varepsilon\mathbb{Z}^2$ we associate the set

$$E_{\mathcal{I}} = \bigcup_{\underline{i} \in \mathcal{I}} Q_\varepsilon(\underline{i}).$$

The space of *admissible sets* related to indices in the two-dimensional square lattice is then defined by

$$\mathcal{D}_\varepsilon := \left\{ E \subseteq \mathbb{R}^2 : E = E_{\mathcal{I}} \text{ for some } \mathcal{I} \subseteq \varepsilon\mathbb{Z}^2 \right\}.$$

We note that the value of the energy $P^\varepsilon(\mathcal{I})$ is the same as the perimeter of the corresponding set $E_{\mathcal{I}} \in \mathcal{D}_\varepsilon$, so that it can be thought as a *discrete perimeter* of \mathcal{I} . With a slight abuse of notation then, we will use the same notation

$$P^\varepsilon(E_{\mathcal{I}}) = P^\varepsilon(\mathcal{I}) = \mathcal{H}^1(\partial E_{\mathcal{I}}). \quad (2.2)$$

Remark 2.1 (Γ -convergence of discrete perimeter energies). The perimeter functionals defined above can be extended to the whole space of sets of finite perimeter in \mathbb{R}^2 by setting

$$P^\varepsilon(E) = \begin{cases} \mathcal{H}^1(\partial E) & \text{if } E \in \mathcal{D}_\varepsilon \\ +\infty & \text{otherwise.} \end{cases}$$

The Γ -limit of these energies in this space with respect to the convergence $|E_j \Delta E| \rightarrow 0$ is given by the *anisotropic perimeter functional* defined as

$$P(E) = \int_{\partial^* E} \|\nu\|_1 \, d\mathcal{H}^1,$$

where $\nu = (\nu_1, \nu_2)$ is the euclidean unit inner normal to $\partial^* E$, and $\|\nu\|_1 = |\nu_1| + |\nu_2|$ (see e.g. [1]).

Note that the constraint $E \in \mathcal{D}_\varepsilon$ is lost in the limit, but the anisotropies of the underlying lattice reappear in the anisotropy energy density $\|\nu\|_1$.

2.2 A discrete-in-time minimization scheme

We will consider a discrete motion obtained by successive minimization of the discrete perimeter functionals and an additional distance term.

For $\mathcal{I} \subset \varepsilon\mathbb{Z}^2$ we define the *discrete L^∞ -distance* from $\partial\mathcal{I}$ as

$$d_\infty^\varepsilon(\underline{i}, \partial\mathcal{I}) = \begin{cases} \inf\{\|\underline{i} - \underline{j}\|_\infty : \underline{j} \in \mathcal{I}\} & \text{if } \underline{i} \notin \mathcal{I} \\ \inf\{\|\underline{i} - \underline{j}\|_\infty : \underline{j} \in \varepsilon\mathbb{Z}^2 \setminus \mathcal{I}\} & \text{if } \underline{i} \in \mathcal{I}, \end{cases}$$

where $\|z\|_\infty = |z_1| \vee |z_2|$. Note that we have

$$d_\infty^\varepsilon(\underline{i}, \partial\mathcal{I}) = d_\infty(\underline{i}, \partial E_{\mathcal{I}}) + \frac{\varepsilon}{2},$$

where d_∞ denotes the usual l^∞ -distance. This distance can be extended to all $\mathbb{R}^2 \setminus \partial E_{\mathcal{I}}$ by setting

$$d_\infty^\varepsilon(x, \partial\mathcal{I}) = d_\infty^\varepsilon(\underline{i}, \partial\mathcal{I}) \text{ if } x \in Q_\varepsilon(\underline{i}).$$

In the following we will directly work with $E \in \mathcal{D}_\varepsilon$, so that the distance can be equivalently defined by

$$d_\infty^\varepsilon(x, \partial E) = d_\infty(\underline{i}, \partial E) + \frac{\varepsilon}{2} \text{ if } x \in Q_\varepsilon(\underline{i}).$$

Note that this is well defined as a measurable function, since its definition is unique outside the union of the boundaries of the squares Q_ε (that are a negligible set).

We now fix a time step τ and introduce a discrete motion with underlying time step τ obtained by successive minimization. At each time step we will minimize an energy $\mathcal{F}_{\varepsilon,\tau} : \mathcal{D}_\varepsilon \times \mathcal{D}_\varepsilon \rightarrow \mathbb{R}$ defined as

$$\mathcal{F}_{\varepsilon,\tau}(E, F) = P^\varepsilon(E) + \frac{1}{\tau} \int_{E \Delta F} d_\infty^\varepsilon(x, \partial F) dx$$

(here we use the continuous formulation of the energies as above). Even though we will find it convenient to use the continuous version of these energies, it must be kept in mind that they can be equally interpreted as defined on pairs of subsets of $\varepsilon\mathbb{Z}^2$, on which they have the form

$$\begin{aligned} \mathcal{F}_{\varepsilon,\tau}(\mathcal{I}, \mathcal{J}) &= P^\varepsilon(\mathcal{I}) + \frac{1}{\tau} \sum_{\underline{i} \in \mathcal{I} \Delta \mathcal{J}} \varepsilon^2 d_\infty^\varepsilon(\underline{i}, \partial\mathcal{J}) \\ &= P^\varepsilon(\mathcal{I}) + \frac{1}{\tau} \left(\sum_{\underline{i} \in \mathcal{I} \setminus \mathcal{J}} \varepsilon^2 d_\infty(\underline{i}, \mathcal{J}) + \sum_{\underline{i} \in \mathcal{J} \setminus \mathcal{I}} \varepsilon^2 d_\infty(\underline{i}, \mathbb{Z}^2 \setminus \mathcal{J}) \right). \end{aligned}$$

Given an initial set $E_{0,\varepsilon}$ we define recursively a sequence $E_{\varepsilon,\tau}^k$ in \mathcal{D}_ε by requiring that:

- (1) $E_{\varepsilon,\tau}^0 = E_{0,\varepsilon}$;
- (2) $E_{\varepsilon,\tau}^{k+1}$ is a minimizer of the functional $\mathcal{F}_{\varepsilon,\tau}(\cdot, E_{\varepsilon,\tau}^k)$.

The *discrete flat flow* associated to functionals $\mathcal{F}_{\varepsilon,\tau}$ is thus defined by

$$E_{\varepsilon,\tau}(t) = E_{\varepsilon,\tau}^{\lfloor t/\tau \rfloor}.$$

Assuming that the initial data $E_{0,\varepsilon}$ tend, for instance in the Hausdorff sense, to a (sufficiently regular) set E , we are interested in identifying the motion described by any converging subsequence of $E_{\varepsilon,\tau}(t)$ as $\varepsilon, \tau \rightarrow 0$.

It will be shown that the interaction between the two discretization parameters, in time and space, plays a relevant role in such a limiting process. More precisely the limit motion depends strongly on their relative decrease rate to 0. Indeed if $\varepsilon \ll \tau$ then we may first let $\varepsilon \rightarrow 0$, so that $P^\varepsilon(E)$ can be directly substituted by the limit anisotropic perimeter $P(E)$ and $\frac{1}{\tau} \int_{E \Delta F} d_\infty^\varepsilon(x, \partial F) dx$ by $\frac{1}{\tau} \int_{E \Delta F} d_\infty(x, \partial F) dx$. As a consequence the approximated flat motions tend to the solution of the continuous ones studied by Almgren and Taylor (see [5]). On the other hand if $\varepsilon \gg \tau$ then there is no motion and $E_{\varepsilon,\tau}^k \equiv E_{0,\varepsilon}$. Indeed, for any $F \neq E_{0,\varepsilon}$ and for τ small enough we have

$$\frac{1}{\tau} \int_{E_{0,\varepsilon} \Delta F} d_\infty^\varepsilon(x, \partial F) dx \geq c \frac{\varepsilon}{\tau} > P^\varepsilon(E_{0,\varepsilon}).$$

In this case the limit motion is the constant state E . An heuristic computation suggests that the meaningful regime is the intermediate case $\tau \sim \varepsilon$. We will study in detail this case, the behaviour in the other regimes being immediately deduced from this analysis.

3 Convergence of the minimization process

3.1 The case of a rectangle

We first treat the case of initial data $E_{0,\varepsilon}$ that are *coordinate rectangles*; i.e., rectangles with sides parallel to the coordinate directions, of lengths $L_{1,\varepsilon}^0, L_{2,\varepsilon}^0$, respectively. Despite its simplicity this case captures all the features of the motion, and can be fruitfully compared with the continuous crystalline motion.

For the sake of simplicity in the sequel we assume that

$$\tau = \alpha\varepsilon \text{ for some } \alpha \in (0, +\infty),$$

and, correspondingly, we omit the dependence on τ in the notation of

$$E_\varepsilon^k = E_{\varepsilon,\tau}^k (= E_{\varepsilon,\alpha\varepsilon}^k).$$

We underline that all the results remains true in the more general case $\lim_{\varepsilon \rightarrow 0+} \frac{\tau}{\varepsilon} = \alpha$ with minor changes in the proofs.

The following characterization of any limit motion holds.

Theorem 3.1 (Quantization of the limit speed). *For all $\varepsilon > 0$, let $E_\varepsilon \in \mathcal{D}_\varepsilon$ be a coordinate rectangle with sides $S_{1,\varepsilon}, \dots, S_{4,\varepsilon}$. Assume also that*

$$\lim_{\varepsilon \rightarrow 0+} d_{\mathcal{H}}(E_\varepsilon, E) = 0$$

for some fixed coordinate rectangle E . Then, up to a subsequence, $E_\varepsilon(t)$ converges as $\varepsilon \rightarrow 0$ locally in time to $E(t)$, where $E(t)$ is a coordinate rectangle

with sides $S_i(t)$, and such that $E(0) = E$. Any S_i moves inward with velocity $v_i(t)$ solving the following differential inclusions

$$v_i(t) \begin{cases} = \frac{1}{\alpha} \left\lfloor \frac{2\alpha}{L_i(t)} \right\rfloor & \text{if } \frac{2\alpha}{L_i(t)} \notin \mathbb{N} \\ \in \left[\frac{1}{\alpha} \left(\frac{2\alpha}{L_i(t)} - 1 \right), \frac{1}{\alpha} \frac{2\alpha}{L_i(t)} \right], & \text{if } \frac{2\alpha}{L_i(t)} \in \mathbb{N} \end{cases} \quad (3.1)$$

where $L_i(t) := |S_i(t)|$ denotes the length of the side $S_i(t)$, until the extinction time when $L_i(t) = 0$.

Proof. The first remark is that coordinate rectangles evolve into sets of the same type. This can be checked recursively, by showing that if E_ε^k is a rectangle and F is a minimizer for the minimum problem for $\mathcal{F}_{\varepsilon,\tau}(\cdot, E_\varepsilon^k)$ then F is a coordinate rectangle.

In order to prove the assertion let $F = F_1 \cup \dots \cup F_m$ be the decomposition of F into its connected components. We first remark that each F_i is a coordinate rectangle contained in E_ε^k . In fact, if we replace each F_i with the minimum coordinate rectangle containing $F_i \cap E_\varepsilon^k$, its energy decreases since its perimeter is not greater than that of F_i and the symmetric difference with E_ε^k decreases as well (see Fig. 1). Furthermore, the decrease is strictly positive if F_i is not contained in E_ε^k or $F_i \cap E_\varepsilon^k$ is not a rectangle. Note additionally that

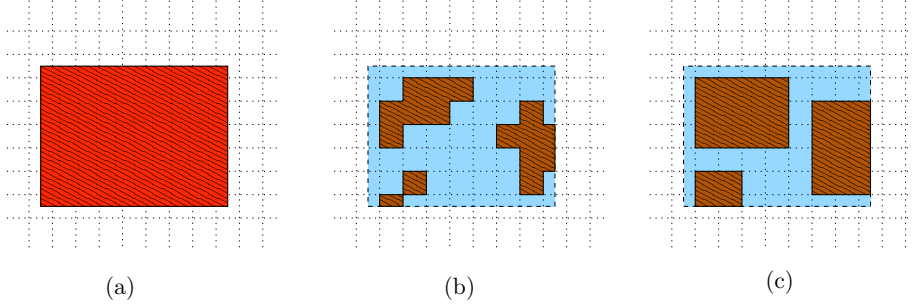


Figure 1: (a) rectangular initial datum, and two possible configurations: the one paying less volume term (c) is preferred

$$d_\infty^\varepsilon(F_i, F_j) \geq \varepsilon, \text{ for } i \neq j.$$

We now prove that actually there is only one connected component. To this end it suffices to prove that each connected component can be translated in direction of the centre of E_ε^k without increasing its energy. Consider then the component F_1 , and denote by P and P' the centers of E_ε^k and F_1 respectively. By a symmetry argument, it is not restrictive to suppose that both components of $P' - P$ are non negative. Moreover we can suppose that $P' \neq P$, since we have at most one connected component of F centered in P . Note that this implies $\|P' - P\|_\infty \geq \varepsilon$. We consider now the set F' obtained by substituting to F_1 the rectangle

$$F'_1 = F_1 - \varepsilon \operatorname{sgn}(\langle P' - P, e_1 \rangle) e_1 - \varepsilon \operatorname{sgn}(\langle P' - P, e_2 \rangle) e_2$$

and this implies that

$$\mathcal{F}_{\varepsilon,\tau}(F \cup \widehat{F}, E_\varepsilon^k) = \mathcal{F}_{\varepsilon,\tau}(F, E_\varepsilon^k) + P^\varepsilon(F) - \frac{1}{\tau} \int_{\widehat{F}} d_\infty^\varepsilon(x, \partial E_\varepsilon^k) dx \leq \mathcal{F}_{\varepsilon,\tau}(F, E_\varepsilon^k).$$

Hence $F \cup \widehat{F}$ is also a minimizer, thus contradicting the connectedness of minimizers proved above. Thus, the recursive minimum process can be performed on coordinate rectangles containing P .

We now can proceed in explicitly computing the minimizer E_ε^1 . Indeed, set $L_{i,\varepsilon} := |S_{i,\varepsilon}|$ and let εN_i be the distance of the side $S_{i,\varepsilon}$ from S_i . We can write the functional $\mathcal{F}_{\varepsilon,\tau}(F, E_\varepsilon)$ in terms of the integer distances N_1, \dots, N_4 from the relative sides, we get that $N_{1,\varepsilon}, \dots, N_{4,\varepsilon}$ are minimizers of the function

$$\begin{aligned} f(N_1, \dots, N_4) &= -2\varepsilon \sum_{i=1}^4 N_i + \frac{\varepsilon}{\alpha} \sum_{i=1}^4 \sum_{k=1}^{N_i} k L_{i,\varepsilon} - \frac{\varepsilon^2}{\alpha} e_\varepsilon \\ &= \varepsilon \sum_{i=1}^4 \left(-2N_i + \frac{1}{\alpha} \frac{N_i(N_i+1)}{2} L_{i,\varepsilon} \right) - \frac{\varepsilon^2}{\alpha} e_\varepsilon, \end{aligned} \quad (3.2)$$

where $0 \leq e_\varepsilon \leq C \max(N_1, \dots, N_4)^3$. In the computation above we have subdivided the rectangle between $S_{i,\varepsilon}$ and S_i in N_i strips indexed by k , for each of which the discrete distance is $k\varepsilon$; the last term is due to the contribution of the bulk term close to the corners of the rectangle F , where two neighboring rectangles between $S_{i,\varepsilon}$ and S_i intersect, and is negligible as $\varepsilon \rightarrow 0$ (see Fig. 3).

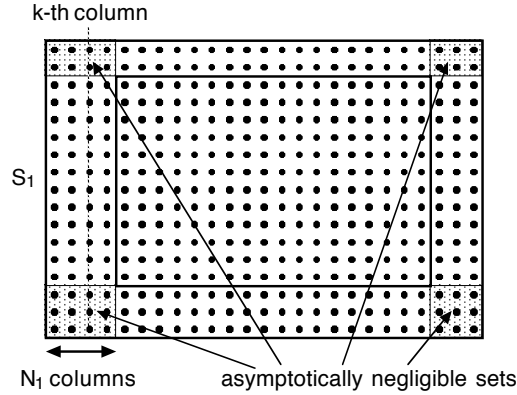


Figure 3: computation of the time-step minimization

The minimizer $N_{1,\varepsilon}, \dots, N_{4,\varepsilon}$ are identified by the inequalities

$$f(\dots, N_{i,\varepsilon}, \dots) \leq f(\dots, N_{i,\varepsilon} \pm 1, \dots).$$

A straight computation shows that $N_{i,\varepsilon}$ is equal to $\lfloor 2\alpha/L_{i,\varepsilon} \rfloor$ except for the “singular” case in which $2\alpha/L_{i,\varepsilon}$ lies in a small neighbourhood of the integers, infinitesimal as $\varepsilon \rightarrow 0$. In this last case there exists a threshold, varying with ε , for which both an integer N and the subsequent $N+1$ are minimizers. More precisely there exists a constant $\bar{C} = C(L_1, \dots, L_4)$ with

$$0 \leq C(L_1, \dots, L_4) \leq \frac{C\alpha^3}{\min(L_1, \dots, L_4)^4}.$$

such that

$$N_{i,\varepsilon} = \left\lfloor \frac{2\alpha}{L_{i,\varepsilon}} \right\rfloor \text{ if } \text{dist}\left(\frac{2\alpha}{L_{i,\varepsilon}}, \mathbb{N}\right) \geq \bar{C}\varepsilon, \quad (3.3)$$

while close to the singular behaviour we only infer that

$$\begin{aligned} N_{i,\varepsilon} &\in \left\{ \left\lfloor \frac{2\alpha}{L_{i,\varepsilon}} \right\rfloor, \left\lfloor \frac{2\alpha}{L_{i,\varepsilon}} \right\rfloor + 1 \right\} \text{ if } \left\lfloor \frac{2\alpha}{L_{i,\varepsilon}} \right\rfloor + 1 - \frac{2\alpha}{L_{i,\varepsilon}} < \bar{C}\varepsilon, \\ N_{i,\varepsilon} &\in \left\{ \left\lfloor \frac{2\alpha}{L_{i,\varepsilon}} \right\rfloor - 1, \left\lfloor \frac{2\alpha}{L_{i,\varepsilon}} \right\rfloor \right\} \text{ if } \frac{2\alpha}{L_{i,\varepsilon}} - \left\lfloor \frac{2\alpha}{L_{i,\varepsilon}} \right\rfloor < \bar{C}\varepsilon. \end{aligned} \quad (3.4)$$

Scaling back these relations, we infer that the side $S_{i,\varepsilon}$ moves inward of a distance $N_{i,\varepsilon}\varepsilon$, with the value of $N_{i,\varepsilon}$ estimated in terms of the quantity $2\alpha/L_{i,\varepsilon}$ as above.

We can iterate this process constructing recursively for $i = 1, \dots, 4$ two sequences $L_{i,\varepsilon}^k, N_{i,\varepsilon}^k$ such that

$$L_{i,\varepsilon}^{k+1} = L_{i,\varepsilon}^k - N_{i-1,\varepsilon}^k \varepsilon - N_{i+1,\varepsilon}^k \varepsilon,$$

with initial conditions $N_{i,\varepsilon}^0 = N_{i,\varepsilon}$ and $L_{i,\varepsilon}^0 = L_{i,\varepsilon}$. $N_{i,\varepsilon}^k$ is a minimizer obtained by the same minimization procedure as above with $L_{i,\varepsilon}^k$ in place of $L_{i,\varepsilon}$. For each $1 \leq i \leq 4$, we then define $L_{i,\varepsilon}(t)$ as the linear interpolation in $[k\tau, (k+1)\tau]$ of the values $L_{i,\varepsilon}^k$.

Note that we have

$$\frac{L_{i,\varepsilon}^{k+1} - L_{i,\varepsilon}^k}{\tau} = -\frac{1}{\alpha}(N_{i-1,\varepsilon}^k + N_{i+1,\varepsilon}^k)$$

so that $L_{i,\varepsilon}(t)$ is a decreasing continuous function of t and the sequence is uniformly Lipschitz continuous on all intervals $[0, T]$ such that $L_{i,\varepsilon}(T) \geq c > 0$. Hence it converges (up to a subsequence) as $\varepsilon \rightarrow 0$ to a function $L_i(t)$, which is also decreasing. It follows that $E_\varepsilon(t)$ converges as $\varepsilon \rightarrow 0$, up to a subsequence and in the Hausdorff sense, to a limit rectangle $E(t)$, for all $t \geq 0$.

It remains to justify rigorously formula (3.1) for the side velocities. For the sake of clarity in the computation we prefer to introduce the piecewise-constant interpolations of the values $L_{i,\varepsilon}^k, N_{i,\varepsilon}^k$. Thus for $t \geq 0$ let $L_i^\tau(t) = L_{i,\varepsilon}^{\lfloor t/\tau \rfloor}$ and $N_i^\tau(t) = N_{i,\varepsilon}^{\lfloor t/\tau \rfloor}$. We have that $L_i^\tau(t) \rightarrow L_i(t)$ locally uniformly as $\tau \rightarrow 0$ and, by continuity, $N_i^\tau(t) \rightarrow v_i(t)$ defined in (3.1) locally uniformly in $\mathbb{R}^+ \setminus \mathbb{N}$ as $\tau \rightarrow 0$.

By construction we also have

$$\begin{aligned} L_i^\tau(t + \tau) &= L_i^0 - \frac{1}{\alpha} \sum_{k=0}^{\lfloor t/\tau \rfloor} \tau(N_{i-1}^\tau(k\tau) + N_{i+1}^\tau(k\tau)) \\ &= L_i^0 - \frac{1}{\alpha} \sum_{k=0}^{\lfloor t/\tau \rfloor} \tau(v_{i-1}(k\tau) + v_{i+1}(k\tau)) + \omega(\tau), \end{aligned}$$

being $\omega(\tau)$ an error infinitesimal as $\tau \rightarrow 0$, where the second equality has been obtained using the convergence of N_i^τ to v_i . Letting $\tau \rightarrow 0$ we infer that

$$L_i(t) = L_i^0 - \frac{1}{\alpha} \int_0^t (v_{i-1}(s) + v_{i+1}(s)) ds,$$

that is equivalent to (3.1) rephrased through the relation $\dot{L}_i(t) = -(v_{i-1}(t) + v_{i+1}(t))$. \square

Theorem 3.2 (Unique limit motions). *Let E_ε, E be as in the statement of Theorem 3.1. Assume in addition that the lengths L_1^0, L_2^0 of the sides of the initial set E satisfy one of the two following conditions (we assume that $L_1^0 \leq L_2^0$):*

- a) $L_1^0, L_2^0 > 2\alpha$ (total pinning);
- b) $L_1^0 < 2\alpha$ and $L_2^0 \leq 2\alpha$ (vanishing in finite time with shrinking velocity larger than $1/\alpha$);
- c) $L_1^0 < 2\alpha$ and $2\alpha/L_1^0 \notin \mathbb{N}$, and $L_2^0 > 2\alpha$ (partial pinning);

then $E_\varepsilon(t)$ converges locally in time to $E(t)$ as $\varepsilon \rightarrow 0$, where $E(t)$ is the unique rectangle with sides of lengths $L_1(t)$ and $L_2(t)$ which solve the following system of ordinary differential equations

$$\begin{cases} \dot{L}_1(t) = -\frac{2}{\alpha} \left\lfloor \frac{2\alpha}{L_2(t)} \right\rfloor \\ \dot{L}_2(t) = -\frac{2}{\alpha} \left\lfloor \frac{2\alpha}{L_1(t)} \right\rfloor \end{cases} \quad (3.5)$$

for a.e. t , with initial conditions $L_1(0) = L_1^0$ and $L_2(0) = L_2^0$.

Proof. From the uniqueness of the ODE in (3.5) we will

In case a) the statement follows by Theorem 3.1 noticing that we have $v_1(t) = v_2(t) = 0$ for all $t \geq 0$, which is equivalent to $\dot{L}_1 = \dot{L}_2 = 0$.

In case b), note that the side length L_2 decrease, with a strictly negative derivative at 0, until it vanishes. The derivative of L_2 , is (minus) twice the velocity v_1 of the side of length L_1 . In particular $\dot{L}_2(t) \leq -2/\alpha$, since $v_1(t) \geq 1/\alpha$ by (3.1), so that in particular $2\alpha/L_2(t) \in \mathbb{N}$ only for a countable number of times t . We can apply the same argument to $L_1(t)$ for all $t > 0$, and get $2\alpha/L_1(t) \notin \mathbb{N}$ for a.e. t . Finally, (3.5) follows straightforwardly from the first equality in (3.1).

In case c), again by (3.1) we infer that the side length L_2 is strictly decreasing until it vanishes, while we have $L_1(t) = L_1^0$ on the interval $[0, T_0]$ characterized by $L_2(T_0) = 2\alpha$. From this, again by (3.1), we deduce that the derivative of L_2 is constant

$$\dot{L}_2(t) = -\frac{2}{\alpha} \left\lfloor \frac{2\alpha}{L_1^0} \right\rfloor$$

in $[0, T_0]$. Hence, at time T_0 we are in the case b), and we can refer to the previous reasoning. \square

Remark 3.3. We point out that (3.1) still holds, with essentially the same proof, if we substitute d_∞ with an equivalent discrete distance.

Under some additional assumptions on the initial side lengths of $E_{0,\varepsilon}$ we may refine the previous result.

Remark 3.4. Condition *a*) gives the ‘pinning threshold’, above which we have no motion, as a condition on the limit initial datum E . A slightly more accurate estimate allows to state the condition on the initial sets E_ε , giving that the same pinning phenomenon occurs if both $L_{i,\varepsilon}^0 > 2\alpha + C\varepsilon$ for some explicitly computable C . A similar remark applies for condition *b*).

3.1.1 Singular initial data

In the cases analyzed in Theorem 3.2 the possible singularities in the limit motions are avoided since either we do not have any motion at all, or the singular points where $2\alpha/L_i$ is integer, so that the velocity of the sides is not uniquely defined, are isolated and hence negligible. It remains then to analyze the cases when neither case *a*) nor *b*) are satisfied. For the sake of simplicity we assume $L_1^0 \leq L_2^0$, and we distinguish two cases:

1. $L_1^0 = L_2^0 = 2\alpha$ (*nonuniqueness*). In this case we can characterize the possible limit motions as follows.

For every $T \in [0, +\infty]$, up to appropriately choosing the initial data E_ε and the discrete motions E_ε^i , we have $v_1(t) = v_2(t) = 0$ for all $t \in [0, T]$, and $v_1(t) = v_2(t) > 0$ for $t > T$ (assuming $T < +\infty$) until the extinction time, as in case *b*) of Theorem 3.2. In particular, the initial square does not move for $t \in [0, T]$, and shrinks homothetically to its centre for $t > T$.

2. $L_1^0 = 2\alpha/N$, with $N \in \mathbb{N}$ and $L_2^0 > 2\alpha$ (*partial pinning*).

Also in this case we lose uniqueness and moreover the limit motion $E(t)$ may not maintain the same center even if all the initial data E_0^ε have the same center. More precisely, there exists $T \in (0, +\infty]$ such that $v_2(t) = v_4(t) = 0$ for all $t \in [0, T]$, and $L_2(T) = 2\alpha$ (assuming $T < +\infty$). If $N = 1$; *i.e.*, $L_1^0 = 2\alpha$, from time T on we are back to case 1 above. If $N > 1$ then T is always finite, and we can reason as in the case *c*) in Theorem 3.2, obtaining a unique motion from that time. We point out that in the time interval $[0, T)$, thanks to the non-uniqueness of the minimizers E_ε^i , for the sides $S_1(t), S_3(t)$ we may obtain all velocities satisfying the bounds $v_i(t) \in (1/\alpha)[N-1, N]$, $i \in \{1, 3\}$. In particular, we can have $v_1(t) \neq v_3(t)$ for a set of positive measure in $[0, T)$, so that the center of the evolving rectangle $E(t)$ may move in the time interval $[0, T]$.

Remark 3.5. Note that in the singular cases described above the motion does depend on the choice of the ‘microscopic’ initial data $E_{0,\varepsilon}$.

3.2 The case of a polyrectangle

In this section we extend the results obtained in the previous section for coordinate rectangles to the case in which the limit initial set is a polyrectangle.

We first introduce the definition of polyrectangle, and we assign a curvature sign on each side (this is quite standard see for instance [5]).

Definition 3.6. We say that E is a (coordinate) polyrectangle if ∂E is locally a Lipschitz graph, and

$$\nu_E \in \{\pm e_1, \pm e_2\} \quad \text{for a.e. } x \in \partial E.$$

For any polyrectangle E we assign to each sides S_i an integer number δ_i (the sign of the curvature of S_i) as follows (see Figure 4): $\delta_i = 1$ (resp. $\delta_i = -1$) if there exists $r > 0$ such that $E \cap (S_i + B_r)$ (resp. $(\mathbb{R}^2 \setminus E) \cap (S_i + B_r)$) is a convex set, we set $\delta_i = 0$ if none of the two conditions holds.

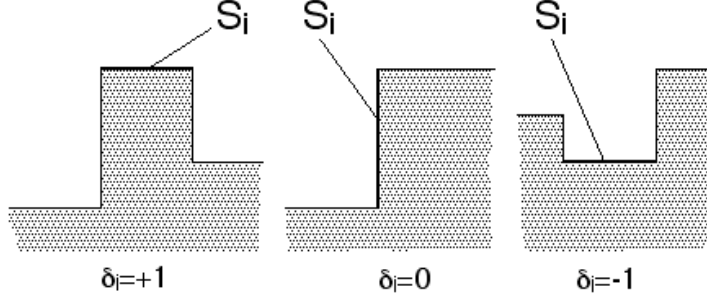


Figure 4: Sides of a polyrectangle with different curvature signs

Remark 3.7. Let F, G be two minimizers of $\mathcal{F}_{\varepsilon, \tau}(\cdot, E)$, then $F \cup G$ and $F \cap G$ are also minimizers. Indeed it suffices to notice that $P_\varepsilon(F) + P_\varepsilon(G) \geq P_\varepsilon(F \cup G) + P_\varepsilon(F \cap G)$ and

$$\begin{aligned} & \frac{1}{\tau} \int_{E \Delta (F \cap G)} d_\infty^\varepsilon(x, \partial E) dx + \frac{1}{\tau} \int_{E \Delta (F \cup G)} d_\infty^\varepsilon(x, \partial E) dx \\ &= \frac{1}{\tau} \int_{E \Delta F} d_\infty^\varepsilon(x, \partial E) dx + \frac{1}{\tau} \int_{E \Delta G} d_\infty^\varepsilon(x, \partial E) dx. \end{aligned}$$

From which we deduce $\mathcal{F}_{\varepsilon, \tau}(F \cap G, E) + \mathcal{F}_{\varepsilon, \tau}(F \cup G, E) \leq \mathcal{F}_{\varepsilon, \tau}(F, E) + \mathcal{F}_{\varepsilon, \tau}(G, E) = 2 \min \mathcal{F}_{\varepsilon, \tau}(\cdot, E)$. As a consequence, the *largest* (respectively the *smallest*) minimizer with respect to inclusion is well defined.

We can now state a *weak comparison principle* for our motion both in the discrete and the limit case.

Proposition 3.8 (discrete weak comparison principle). *Let $\varepsilon > 0$ and let $R_\varepsilon, K_\varepsilon \in \mathcal{D}_\varepsilon$ be such that $R_\varepsilon \subseteq K_\varepsilon$ and R_ε is a coordinate rectangle. Let K_ε^k be a motion from K_ε constructed by successive minimizations. Then, $R_\varepsilon^k \subseteq K_\varepsilon^k$ for all $k \geq 1$, where R_ε^k is a motion from R_ε constructed by successively choosing a minimizer of $\mathcal{F}_{\varepsilon, \tau}(\cdot, R_\varepsilon^{k-1})$ having smallest measure.*

Proof. As usual it is enough to prove the statement for $k = 1$. We claim that

$$\mathcal{F}_{\varepsilon, \tau}(K_\varepsilon^1 \cup R_\varepsilon^1, K_\varepsilon) \leq \mathcal{F}_{\varepsilon, \tau}(K_\varepsilon^1, K_\varepsilon).$$

Since R_ε^1 is a minimizer for $\mathcal{F}_{\varepsilon, \tau}(\cdot, R_\varepsilon)$, we have

$$\begin{aligned} & \mathcal{F}_{\varepsilon, \tau}(K_\varepsilon^1 \cap R_\varepsilon^1, R_\varepsilon) - \mathcal{F}_{\varepsilon, \tau}(R_\varepsilon^1, R_\varepsilon) \\ &= P^\varepsilon(K_\varepsilon^1, R_\varepsilon^1) - \mathcal{H}^1((\partial R_\varepsilon^1) \setminus K_\varepsilon^1) + \frac{1}{\tau} \int_{R_\varepsilon^1 \setminus K_\varepsilon^1} d_\infty^\varepsilon(x, \partial R_\varepsilon) dx \geq 0, \end{aligned}$$

where $P^\varepsilon(A, B)$ denotes the relative perimeter of A in B . Moreover taking into account that R_ε^1 is a minimizer with minimal measure, the equality holds if and only if $K_\varepsilon^1 \cap R_\varepsilon^1 = R_\varepsilon^1$. Note also that for $x \in R_\varepsilon$ $d_\infty^\varepsilon(x, \partial R_\varepsilon) \leq d_\infty^\varepsilon(x, \partial K_\varepsilon)$, which implies that

$$\begin{aligned} & \mathcal{F}_{\varepsilon, \tau}(K_\varepsilon^1, K_\varepsilon) - \mathcal{F}_{\varepsilon, \tau}(K_\varepsilon^1 \cup R_\varepsilon^1, K_\varepsilon) \\ &= P^\varepsilon(K_\varepsilon^1, R_\varepsilon^1) - \mathcal{H}^1((\partial R_\varepsilon^1) \setminus K_\varepsilon^1) + \frac{1}{\tau} \int_{R_\varepsilon^1 \setminus K_\varepsilon^1} d_\infty^\varepsilon(x, \partial K_\varepsilon) dx \\ &\geq \mathcal{F}_{\varepsilon, \tau}(K_\varepsilon^1 \cap R_\varepsilon^1, R_\varepsilon) - \mathcal{F}_{\varepsilon, \tau}(R_\varepsilon^1, R_\varepsilon) \geq 0 \end{aligned}$$

as desired. \square

Remark 3.9. Notice that the set $\mathbb{R}^2 \setminus K_\varepsilon^k$ is the k -step evolution of the complementary $\mathbb{R}^2 \setminus K_\varepsilon^k$ of K_ε . As a consequence, if we have $R_\varepsilon \subseteq \mathbb{R}^2 \setminus K_\varepsilon$ from Proposition 3.8 it follows $R_\varepsilon^k \subseteq \mathbb{R}^2 \setminus K_\varepsilon^k$, for all $k \geq 1$.

Corollary 3.10 (continuous weak comparison principle). *Let $K \subseteq \mathbb{R}^2$ be fixed and let R be a coordinate rectangle included in the interior part of K . For any $\varepsilon > 0$ let $K_\varepsilon \in \mathcal{D}_\varepsilon$ be such that $K_\varepsilon(t)$ converges to a limit motion $K(t)$ with $K(0) = K$. Then, for any $t \geq 0$ $K(t) \supseteq R(t)$, where $R(t)$ is the limit motion associated to any sequence R_ε of coordinate rectangles such that $d_{\mathcal{H}}(R_\varepsilon, R) \rightarrow 0$, $R_\varepsilon \subseteq R$ and R_ε^k is obtained inductively by choosing the minimizer with smallest measure.*

Theorem 3.11 (motion of polyrectangles). *Let E be a connected bounded polyrectangle with sides S_1, \dots, S_N . For $\varepsilon > 0$ let $E_\varepsilon \in \mathcal{D}_\varepsilon$ be connected polyrectangles, with sides $S_{1, \varepsilon}, \dots, S_{N, \varepsilon}$, such that $\lim_{\varepsilon \rightarrow 0} d_{\mathcal{H}}(E_\varepsilon, E) = 0$. Then, there exists $T > 0$ such that $E_\varepsilon(t)$ converges, (up to a subsequence) as $\varepsilon \rightarrow 0$, in the Hausdorff topology and locally uniformly on $[0, T)$, to a polyrectangle $E(t)$, with $E(0) = E$. Moreover, the sides $S_i(t)$ of $E(t)$, $1 \leq i \leq N$, move with velocity $v_i(t)$ solving the following differential inclusions*

$$v_i(t) \begin{cases} = \frac{\delta_i}{\alpha} \left\lfloor \frac{2\alpha}{L_i(t)} \right\rfloor & \text{if } \frac{2\alpha}{L_i(t)} \notin \mathbb{N} \\ \in \left[\frac{\delta_i}{\alpha} \left(\frac{2\alpha}{L_i(t)} - 1 \right), \frac{\delta_i}{\alpha} \frac{2\alpha}{L_i(t)} \right] & \text{if } \frac{2\alpha}{L_i(t)} \in \mathbb{N}, \end{cases} \quad (3.6)$$

where $L_i(t) = |S_i(t)|$, as before. As a consequence, if we further assume that $2\alpha/L_i^0 \notin \mathbb{N}$ for all $1 \leq i \leq N$, the lengths $L_i(t)$ solve the following system of ODEs

$$\dot{L}_i(t) = - \left(\frac{\delta_{i-1}}{\alpha} \left\lfloor \frac{2\alpha}{L_{i-1}(t)} \right\rfloor + \frac{\delta_{i+1}}{\alpha} \left\lfloor \frac{2\alpha}{L_{i+1}(t)} \right\rfloor \right). \quad (3.7)$$

The time $T > 0$ can be chosen as the first time for which $\lim_{t \rightarrow T} L_i(t) = 0$, for some $i \in \{1, \dots, N\}$.

Proof. We start by proving that each E_ε^k remains connected. As usual it is enough to prove the result for $k = 1$. To do this we first need an estimate

on the volume of the “small components” of E_ε^1 that we obtain by using the comparison principle. Let $\ell > 0$ be the maximum number such that for each point $x \in E$ there exists $y \in \mathbb{R}^2$ such that $x \in (y + Q_\ell) \subseteq E$, where $Q_\ell = [-\ell/2, \ell/2] \times [-\ell/2, \ell/2]$ and the same property holds for $x \notin E$. Up to choosing a small ℓ we may assume that the property holds also for any E_ε . By applying Proposition 3.8 and Remark 3.9 to the union of cubes contained in each E_ε , and to those outside E_ε , respectively, and taking into account (3.3) it follows that

$$d_{\mathcal{H}}(\partial E_\varepsilon^1, \partial E_\varepsilon) \leq \left(\frac{2\alpha}{\ell} + 1 \right) \varepsilon. \quad (3.8)$$

Assume by contradiction that E_ε^1 is not connected and decompose $E_\varepsilon^1 = E_{0,\varepsilon}^1 \cup \cup_{i=1}^N E_{i,\varepsilon}^1$ with $E_{0,\varepsilon}^1$ the component containing all the points of E_ε having distance more than $C'\varepsilon$ from ∂E_ε for a suitable $C' < 2\alpha/\ell + 1$. Therefore for a suitable constant C'' we have

$$d_\infty^\varepsilon(x, \partial E_\varepsilon) \leq C''\varepsilon \quad \text{for all } x \in E_{i,\varepsilon}^1 \text{ and } i \geq 0. \quad (3.9)$$

By using the isoperimetric inequality, for ε small enough we infer

$$\frac{1}{\tau} \int_{E_{i,\varepsilon}^1} d_\infty^\varepsilon(x, \partial E_\varepsilon) dx \leq (C''/\alpha) |E_{i,\varepsilon}^1| < C_{\text{iso}} \sqrt{|E_{i,\varepsilon}^1|} \leq P_\varepsilon(E_{i,\varepsilon}^1),$$

with C_{iso} being the constant of the isoperimetric inequality. Thus, we get a contradiction since we can decrease (strictly) the energy by considering the set $E' = E_{0,\varepsilon}^1$ as a competitor.

The rest of the proof closely follows the arguments in [5] so we only give a sketch of it. We preliminary note that it is not restrictive to assume that for any $\varepsilon > 0$ the curvature signs of the sides $S_{i,\varepsilon}$ coincide with those of the initial polyrectangle E . The first claim is that the sides of E_ε^1 are obtained by those of E_ε by moving each side $S_{i,\varepsilon}$ in direction parallel to the inner normal to the side itself with coefficient δ_i , of distance at most $C\varepsilon$ of the sides of E_ε . Roughly speaking we claim that sides with curvature 0 does not move (even if their lengths may decrease), sides with positive curvature moves inwards, while the opposite happens for sides with negative curvature. Once the claim is established we infer that at each iteration the number of sides remains unchanged and it remains to compute the modulus of the velocity of each side. This will be done performing a computation similar to the one in the proof of Theorem 3.1.

We are left with proving the claim. Since the boundary of E_ε^1 satisfies (3.9) we will reason locally and prove that in a neighbourhood of each side S_i this set consists of a segment parallel to S_i plus two orthogonal segments. We first deal with the case $\delta_i = 1$. Let U_ε^i be the $C''\varepsilon$ -neighbourhood of S_i as shown in Fig. 5. We can assume that $E_\varepsilon^1 \cap U_\varepsilon^i \subseteq E_\varepsilon$ otherwise we can replace E_ε^1 with $E_\varepsilon^1 \setminus (U_\varepsilon^i \setminus E_\varepsilon)$ strictly decreasing the energy. Assume a coordinate system to be fixed as shown in Fig. 5 and let P_1, P_2, P_3 be three points in ∂E_ε^1 such that P_1 has maximum y -coordinate, while P_2 and P_3 are chosen in order to have x -coordinate minimum and maximum, respectively, and maximum y -coordinate. Let also \hat{r} be the horizontal line passing through P_1 (see Fig. 5 (a)). We now construct another competitor E'' whose boundary differs from that of E_ε^1 by substituting the curve having P_2 and P_3 as endpoints and lying in U_ε^i with the two vertical segments connecting P_2 and P_3 with \hat{r} plus the related horizontal

segment (see Fig. 5 (b)). It is easily checked that in case E'' differs from E_ε^1 the functional value strictly improves, contradicting the minimality of E_ε^1 . Hence the boundary of E_ε^1 must coincide with that of E'' and the claim is proved. Analogously one may deal with the remaining cases.

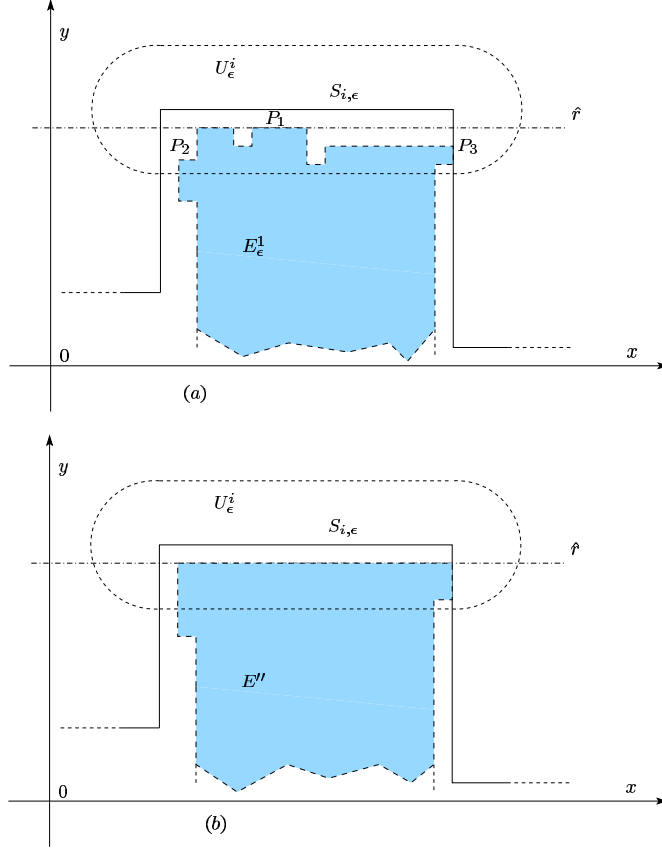


Figure 5: A competitor and its improved version

Finally, let $S_{i,\varepsilon}^1$ be the side of E_ε^1 corresponding to $S_{i,\varepsilon}$ and let $\delta_i N_{i,\varepsilon}$ be its distance from $S_{i,\varepsilon}$. The values of $N_{i,\varepsilon}$ can be obtained performing a computation analogous to the one in the proof of Theorem 3.1, locally for each side. The thesis now follows passing to the limit as in Theorems 3.1 and repeating the reasoning in 3.2 for the uniqueness of the limit motion. \square

Example 3.12 (*polyrectangular (non-convex) pinned sets*). Consider the initial set

$$E = ([-R_1, R_1] \times [-R_2, R_2]) \cup ([-R_2, R_2] \times [-R_1, R_1]),$$

where $\alpha < R_1 < R_2$ (the set on the left in Fig. 6). Then the sides S_i of E either have curvature of sign 0, or length larger than 2α so that $\dot{L}_i = 0$ in the previous theorem, and $E(t) = E$ for all times.

Another example is the set on the right in Fig. 6. Note that this set is not even *geodesically convex* with respect to the distance related to the l^1 -norm

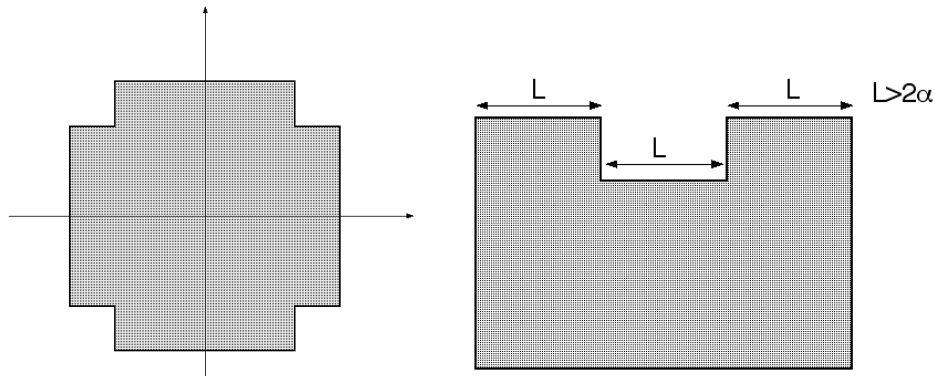


Figure 6: non-convex pinned sets

(i.e., not all pairs of points are connected by a minimal path with respect to that distance), while the first one is.

Example 3.13 (*pinning after an initial motion*). Consider as initial set a square of side length larger than 2α from which a small square has been removed (see Fig. 7). Then the larger boundary stays pinned while the inner square shrinks

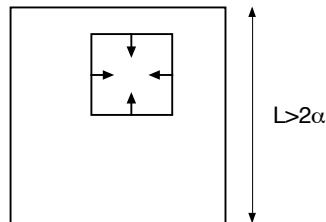


Figure 7: pinning after an initial motion

to a point after a finite time. After that time the motion is constant (equal to the larger square).

3.3 Evolution of more general sets

While the study of the motion of rectangular and polyrectangular sets already contains the main technical features of more general motions, some phenomena can be highlighted only by considering a larger class of sets.

3.3.1 A case study

We begin this section with a case study, when the initial set is a rhombus (more precisely, a coordinate square rotated by 45 degrees). From the proof it will be clear that the same characterization of the motion holds for initial sets that are convex and symmetric with respect to both axes. In the next section we will then show how the same conclusions can be drawn for more general convex initial sets.

We consider the (limit) initial set

$$E = \{(x, y) : |x| + |y| \leq R_0\};$$

i.e., the square with diagonals the segments on the coordinate axes centered in 0 and of length $2R_0$. The initial sets for the discrete motions are

$$E_\varepsilon = \bigcup \{Q_\varepsilon(i) : Q_\varepsilon(i) \subset E\}.$$

Example 3.14 (*a first characterization of the limit motion*). As for the case of rectangular sets we can show that the successive minimization process from E_ε gives sets E_ε^k which are connected, and furthermore they coincide with the intersection of a coordinate rectangle and E_ε .

The second statement follows by induction assuming that $E_\varepsilon^k = R^k \cap E_\varepsilon$ for some rectangle R^k (this clearly holds for $E_\varepsilon^0 = E_0$). We can define R^k as the minimal such rectangle. First note that $E_\varepsilon^{k+1} \subset E_\varepsilon^k$, otherwise we get a contradiction to the minimality by considering $E_\varepsilon^{k+1} \cap E_\varepsilon^k$ in its place, as for the case of rectangles. Let F be a connected component of E_ε^{k+1} then we can consider the minimal coordinate rectangle R containing F . Note that the perimeter of R is not greater than that of F , and equal to that of $R \cap E_\varepsilon$. Moreover, since $F \subset E_\varepsilon^k = R^k \cap E_\varepsilon$, then $R \subset R^k$ and $R \cap E_\varepsilon = R \cap E_\varepsilon^k$. We can conclude then that $F = R \cap E_\varepsilon^k$, otherwise we could replace it with $R \cap E_\varepsilon^k$ and strictly decrease the energy.

The reasoning above shows that each connected component of E_ε^{k+1} is the intersection of a rectangle with E_ε . The induction argument is then completed if we show that we indeed have only one connected component. To this end we can repeat the same translation argument as for rectangular sets. In fact, if $F = R \cap E_\varepsilon^k$ is a connected component not containing 0 and P is its center, we can assume $\langle P, e_i \rangle > 0$ and consider the set

$$G = ((E_\varepsilon^{k+1} \setminus F) \cup (R - \varepsilon e_i)) \cap E_\varepsilon^k$$

in which we substitute $(R - \varepsilon e_i) \cap E_\varepsilon^k$ to F (see Fig. 8).

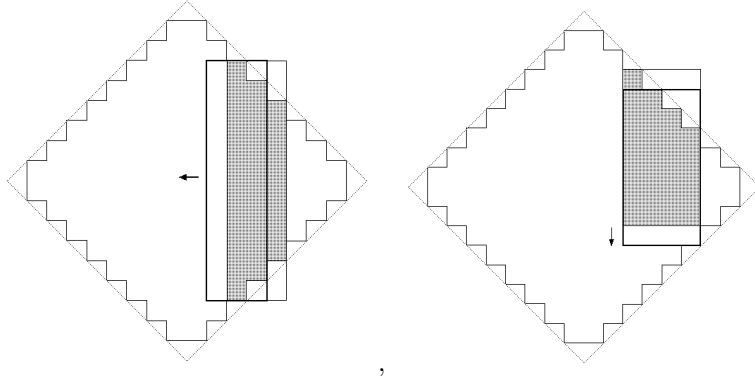


Figure 8: translation argument for a rhombus

As for the case of rectangles, G does not increase the energy and results in a translation of a connected component towards the centre. If E_ε^{k+1} is composed of

more than one connected component then this process, applied a finite number of steps produces a competitor which strictly decreases the energy, contradicting its minimality.

Remark 3.15 (*partial pinning of the boundary*). As a first interesting remark we note that, since the motion of the sets is continuous in the L^1 norm, if a limit motion exists then by the characterization above is of the form

$$E(t) = R(t) \cap E,$$

with $R(t)$ a family of rectangles with $R(0) = [-R_0, R_0]^2$ continuously varying with t . This shows that the motion proceeds at the start only as the motion of four sides with normal coordinate vectors which move inwards from the corners of the rhombus. The original sides of the rhombus do not move inwards (pinning), but decrease in length due to the motion of the other four sides.

Note that, for $\varepsilon > 0$ fixed, we can consider the datum E_ε as a polyrectangle. For such E_ε the sides of the rhombus correspond to sides with curvature of zero sign, except for the endpoints, so that this pinning phenomenon is coherent with the study in the previous section.

Remark 3.16 (*total pinning after an initial motion*). By Proposition 3.8 we can compare the motion $E(t)$ with the motion of each cube contained in E . In particular, if the side R_0 is large enough, we will have cubes contained in E for which the motion is trivial. Hence the set $E(t)$ will contain the union C_0 of all such cubes for all times. The motion is then pinned by this set. Note that this set is not a polyrectangle (see Fig. 9).

We can now explicitly characterize the motion of the rhombus in dependence of its initial side length.

Example 3.17. We first note that the overall motion is completely characterized by the motion of the four sides with normal a coordinate vector. Moreover, due to the pinning of the other sides, this motion is completely localized. We additionally remark that for the discrete motion the sides originated from the corner points do move (for the results on the motion of polyrectangles in the previous section). Let $L(t)$ be the length of one of such sides (we will see that all the sides will have equal length at a time t). In this case we can repeat the same computation as for the case of a rectangle (to avoid infinite velocity it suffices to characterize this motion with initial length L_0 for $L_0 > 0$ arbitrary small and then let $L_0 \rightarrow 0$). If $s(t)$ is the distance of the side from the origin, this gives

$$\dot{s}(t) = -\frac{1}{\alpha} \left\lfloor \frac{2\alpha}{L(t)} \right\rfloor$$

with the constraint that the endpoints of the side lie on the original sides of the rhombus. Note that the set where the right-hand side is a strictly positive integer are negligible. This characterization is valid until either the sides meet, or the velocity is 0; *i.e.*, $L(t) = 2\alpha$. Before the sides meet we have the relation $s(t) + \frac{L(t)}{2} = R_0$, from which $\dot{L} = -2\dot{s}(t)$, so that we obtain

$$\dot{L}(t) = \frac{2}{\alpha} \left\lfloor \frac{2\alpha}{L(t)} \right\rfloor, \text{ with initial datum } L(0) = 0. \quad (3.10)$$

We then have the following three cases (pictured in Fig. 9).

1) (final pinning of a large rhombus). If $R_0 > \sqrt{2}\alpha$ then the sides move inward with their length non-decreasing and obeying the law given by (3.10) for all times. In particular if T_0 is the first time when $L(T_0) = 2\alpha$ then for $t \geq T_0$ the set $E(t)$ is the octagon with the four sides with normal a coordinate vector of length 2α . This set can be seen as the union of all cubes of side length larger than 2α contained in E as noticed in Remark 3.16;

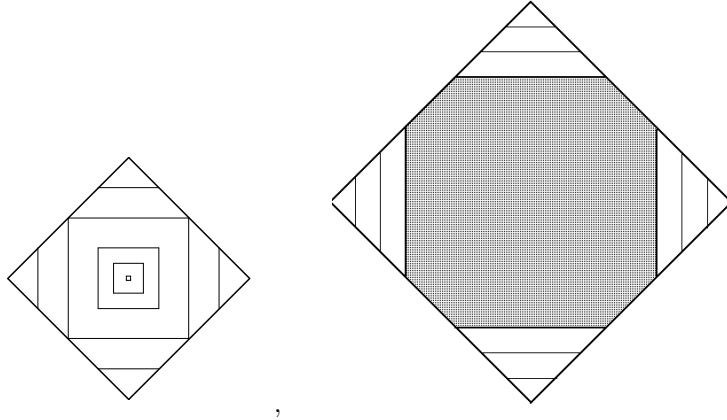


Figure 9: motion of a small and a large rhombus

2) (final extinction of a small rhombus). If $R_0 < \sqrt{2}\alpha$ then the side length follows the law given by (3.10) until the first time T_1 when $L(T_1) = \sqrt{2}R_0$. At this time the motion becomes that of a square of initial side length $\sqrt{2}R_0 < 2\alpha$, already described, which shrinks to 0 in finite time;

3) (non-uniqueness). If $R_0 = \sqrt{2}\alpha$ then at the time T_1 the side length of the limit square is exactly 2α , for which, according to the initial data E_ε , we can have a motion as described in points 1) and 2) above, or we can have $E(t)$ constant on an interval $[T_1, T_2]$ before shrinking to 0 according to point 2).

Remark 3.18 (symmetric convex sets). Note that the reasonings above apply to any convex set which is symmetric with respect to both coordinate axes, and the motion of its sides can be explicitly characterized. We point out that, in this case, if the evolving set is not pinned then it becomes rectangular in finite time, and the symmetry may be lost in the subsequent evolution (see Fig. 10) if the rectangular motion falls in the case of non-uniqueness highlighted in Section 3.1.1.

3.3.2 The convex case

In this section we extend the previous results to a larger class of convex initial sets, where we may apply the translation arguments exemplified in the case of a rhombus leading to the proof of the connectedness of the evolution, and then to its characterization as being the intersection of a rectangle and the initial set for all times. This class will comprise all convex smooth sets. We remark that

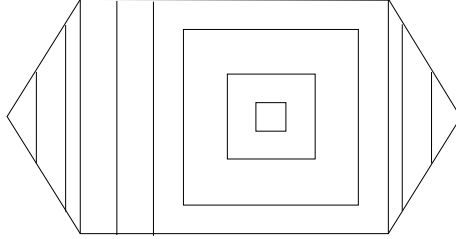


Figure 10: non-symmetric evolution of a symmetric initial set

the arguments below may be generalized to a larger class of sets in the spirit of the extension from rectangular to polyrectangular initial data. However, we leave that (rather complex to state) generalization to the interested reader, as it seems not to bring more information about the nature of the motion.

We first introduce a suitable subclass of convex sets.

Definition 3.19. *Let C be a convex set with non-empty interior, and for all $x \in \partial C$, define $N(x)$ as the blow-up cone of C at x*

$$N(x) = \bigcup_{t \geq 0} t(C - x) .$$

We say that C is a crystalline convex set if for all $x \in \partial C$ the following condition holds:

- (*) *either $\text{int}(N(x))$ contains one of the four coordinate vectors $\pm e_i$, $i \in \{1, 2\}$, or ∂C contains a horizontal or a vertical segment having x as extremal point.*

We point out that (*) is a technical assumption needed to prove the connectedness of the discretized evolution of C , using a translation argument as in the proof of Theorem 3.1. In particular, condition (*) allows us to move in the horizontal or vertical direction small connected components of the minimizing set, which are close to the point x (see Fig. 11 for an example of convex sets not satisfying condition (*)).

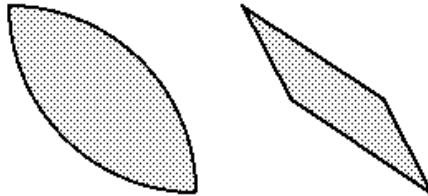


Figure 11: non crystalline convex sets

Theorem 3.20. *Let C be a compact crystalline convex set. For $\varepsilon > 0$, let $C_\varepsilon = \cup_i \{Q_\varepsilon(i) : Q_\varepsilon(i) \subset C\}$. Then, there exists $T > 0$ such that $C_\varepsilon(t)$ converges, (up*

to a subsequence) as $\varepsilon \rightarrow 0$, in the Hausdorff topology and locally uniformly on $[0, T)$, to a crystalline convex set $C(t)$, with $C(0) = C$, and such that

$$C(t) = \bigcap \{C \cap R : R \text{ coordinate rectangle, and } C(t) \subseteq R\} \quad (3.11)$$

for all $t \geq 0$.

Proof. The idea of the proof follows the same lines as that in the proofs of Theorems 3.1 and 3.11. The main difference is that in this general case the Hausdorff distance between the initial (discretized) set C_ε and the minimizer at first step C_ε^1 cannot be estimated as in (3.8) and (3.9) since we cannot choose ℓ independent of ε . As a consequence we cannot repeat the procedure of the proof of Theorem 3.11 to infer the connectedness of the minimizer C_ε^1 . Nevertheless we adapt that technique by choosing ℓ_ε in place of ℓ of the type ε^γ for $0 < \gamma < 1$ (an heuristic consideration suggests $\gamma \sim 1/2$). The main drawback is that the union of such interior cubes does not cover satisfactorily the set C_ε^1 . More precisely, by convexity, an area of order $\varepsilon^{2\gamma}$ can be concentrated in a neighbourhood of the four points with possibly infinite curvature. We overcome this difficulty by a careful choice of γ so that in the end we can decompose C_ε^1 in a bigger connected component containing the evolution of the union of cubes (see (3.12)) and a remaining part with infinitesimal area (see (3.13)). The rest of the proof takes advantage of the translation procedure introduced in the proof of Theorem 3.1 and here the technical request (*) plays also a role.

We divide the proof into three steps.

Step 1. C_ε^1 is a connected subset of C_ε .

We first notice that $C_\varepsilon^1 \subseteq C_\varepsilon$. Indeed it is enough to consider the set $C_\varepsilon^1 \cap C_\varepsilon$: the volume clearly decreases and the same holds for the perimeter thanks to the fact that C_ε is the discretization of a convex set (in particular any external curve made by vertical and horizontal segments connecting two points of ∂C_ε has length not smaller than the one determined by the path along ∂C_ε).

Fix now $\gamma \in (1/3, 1/2)$. Note preliminarily that by (3.3) we can estimate that the side length of the cube $Q_{\varepsilon^\gamma}^1$ obtained by the minimization process from Q_{ε^γ} is larger than $\varepsilon^\gamma - C\varepsilon^{1-\gamma}$. We then apply Proposition 3.8 to the union of cubes of type $x + Q_{\varepsilon^\gamma}$ contained in C_ε and get that

$$\tilde{C}_\varepsilon := \bigcup_{x+Q_{\varepsilon^\gamma} \subset C_\varepsilon} (x + Q_{\varepsilon^\gamma - C\varepsilon^{1-\gamma}}) \subseteq \bigcup_{x+Q_{\varepsilon^\gamma} \subset C_\varepsilon} (x + Q_{\varepsilon^\gamma}^1) \subseteq C_\varepsilon^1. \quad (3.12)$$

Notice that, since C_ε is connected, the set \tilde{C}_ε is also connected. Denoting by $C_{0,\varepsilon}^1$ the connected component of C_ε^1 which contains \tilde{C}_ε , we want to show that $C_{0,\varepsilon}^1 = C_\varepsilon^1$. Using the arguments at the beginning of the section in the case of a rhombus one easily gets that each connected component of C_ε^1 coincides with its rectangular envelope in C_ε , defined for a set A as $C_\varepsilon \cap \{R : R \text{ coordinate rectangle, and } A \subseteq R\}$.

Assume by contradiction that there exists a component $C_{1,\varepsilon}^1 \neq \emptyset$.

We now subdivide the set $C_\varepsilon \setminus \tilde{C}_\varepsilon$ in the two sets

$$A_\varepsilon = \{x \in C_\varepsilon \setminus \tilde{C}_\varepsilon : d_\infty^\varepsilon(x, \partial C_\varepsilon) \leq C\varepsilon^\gamma\},$$

$$B_\varepsilon = \{x \in C_\varepsilon \setminus \tilde{C}_\varepsilon : d_\infty^\varepsilon(x, \partial C_\varepsilon) \leq C\varepsilon^{1-\gamma}\}.$$

To estimate the measure of A_ε we can write

$$|A_\varepsilon| = |A_\varepsilon \setminus C_\varepsilon^1| + |A_\varepsilon \cap C_\varepsilon^1| \leq C'' \varepsilon^{2\gamma} + C''' \varepsilon^{1-\gamma}.$$

where we have used the convexity hypothesis to estimate $|A_\varepsilon \setminus C_\varepsilon^1|$. As for B_ε , we will simply use the estimate $|B_\varepsilon| \leq C \mathcal{H}^1(\partial C_\varepsilon) \varepsilon^{1-\gamma}$. Summarizing, we get that there exists $C' > 0$ such that the following estimates hold:

$$|A_\varepsilon| \leq C' \varepsilon^{2\gamma} \quad |B_\varepsilon| \leq C' \varepsilon^{1-\gamma}.$$

By comparing C_ε^1 with $C_\varepsilon^1 \setminus C_{1,\varepsilon}^1$, and using the fact that $C_{1,\varepsilon}^1 \subset C_\varepsilon \setminus \tilde{C}_\varepsilon$, we deduce this additional estimate on the perimeter of $C_{1,\varepsilon}^1$:

$$\mathbb{P}^\varepsilon(C_{1,\varepsilon}^1) \leq \frac{C}{\varepsilon} \left(\int_{C_{1,\varepsilon}^1 \cap A_\varepsilon} d_\infty^\varepsilon(x, \partial C_\varepsilon) dx + \int_{C_{1,\varepsilon}^1 \cap B_\varepsilon} d_\infty^\varepsilon(x, \partial C_\varepsilon) dx \right) \quad (3.13)$$

$$\leq \frac{C}{\varepsilon} \varepsilon^\gamma |A_\varepsilon| + \frac{C}{\varepsilon} \varepsilon^{1-\gamma} |B_\varepsilon| \leq C (\varepsilon^{3\gamma-1} + \varepsilon^{1-2\gamma}) \leq C(\beta) \varepsilon^\beta, \quad (3.14)$$

for any $0 < \beta < \min(3\gamma - 1, 1 - 2\gamma)$. Therefore from the previous inequality it follows that $C_{1,\varepsilon}^1$ is contained in a coordinate square of side length $C(\beta) \varepsilon^\beta/2$. Once we know that $C_{1,\varepsilon}^1$ is small, recalling that the initial set C satisfies property (*), we can translate $C_{1,\varepsilon}^1$ of ε -steps, either in the horizontal or in the vertical direction, so that the distance $d_\infty^\varepsilon(\cdot, \partial C_\varepsilon)$ is nondecreasing pointwise on $C_{1,\varepsilon}^1$, which implies that the volume term is nondecreasing at each step. The process ends when $C_{1,\varepsilon}^1$ touches one of the other connected components. At this point we can substitute the two components with their rectangular envelope, in such a way that the functional value strictly decreases. This contradicts the minimality of C_ε^1 , hence C_ε^1 is connected.

Step 2. From the previous discussion it follows that

$$C_\varepsilon^1 = C_\varepsilon \cap R_\varepsilon^1, \quad (3.15)$$

where

$$R_\varepsilon^1 = \cap \{R : R \text{ coordinate rectangle, and } C_\varepsilon^1 \subseteq R\}.$$

As a consequence, we can iterate the arguments in the previous step replacing the set C_ε with C_ε^1 , which corresponds to the discretization of the crystalline convex set $C \cap R_\varepsilon^1$. In this way we obtain, for any $k \in \mathbb{N}$, that the sets C_ε^k are connected and

$$C_\varepsilon^k = C_\varepsilon^k \cap \{R : R \text{ coordinate rectangle, and } C_\varepsilon^k \subseteq R\}.$$

The thesis then follows passing to the limit as $\varepsilon \rightarrow 0$. \square

3.3.3 A necessary condition for pinning

We include a necessary condition for pinned sets, which is an immediate consequence of what seen above. It states that the ‘sides’ of a pinned set which have as normal a coordinate vector cannot be shorter than 2α .

Proposition 3.21. *Let E be a Lipschitz initial set such that the corresponding limit motion is constant $E(t) = E$. Then the connected parts of the boundary where one of the components attains a local maximum or minimum must have length larger or equal than 2α .*

Proof. The proof follows immediately by a local comparison close to the sides with a rectangular motion. \square

Remark 3.22 (*conditions for final pinning*). A sufficient condition for sets to be eventually pinned is to contain a square of side length strictly larger than 2α . The motion of such a square is trivial, and hence by comparison is always contained in the evolution.

This is a necessary and sufficient condition for (smooth) convex initial sets, but is far from being necessary for general sets. One example is given by set as in Fig. 7. Note that the difference of the side lengths of the interior and exterior square can be made arbitrarily small.

An example of a simply connected set that gets eventually pinned is given by Fig. 12 (where we take $S < \alpha/2$ and η small enough).

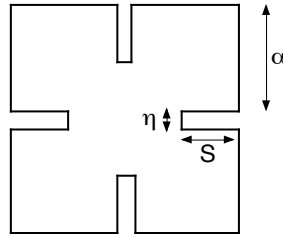


Figure 12: a set pinned to a square after an initial motion

3.3.4 Pinning and de-pinning

From the results above we deduce that the regime $\varepsilon \sim \tau$ is the critical scaling separating the pinning and de-pinning regimes, in the sense that for other scalings either all bounded initial sets shrink to a point in finite time, or all (sufficiently regular) initial sets have a trivial motion.

Theorem 3.23 (pinning and de-pinning). (1) *If $\tau = \tau(\varepsilon)$ is such that*

$$\lim_{\varepsilon \rightarrow 0^+} \frac{\tau}{\varepsilon} = +\infty$$

then all motions $E(t)$ with $E(0)$ bounded shrink to a point after a finite time;

(2) *If $\tau = \tau(\varepsilon)$ is such that*

$$\lim_{\varepsilon \rightarrow 0^+} \frac{\tau}{\varepsilon} = 0$$

then all motions $E(t)$ with $E(0)$ bounded and Lipschitz are trivial: $E(t) = E(0)$.

Proof. (1) follows from a comparison argument with a cube C containing $E(0)$ and $\tau = \alpha\varepsilon$ for α sufficiently large so that C shrinks to a point. To obtain (2) it suffices to fix $\tau = \alpha\varepsilon$ and note that the motion of the polyrectangle E_ε (E_ε an approximation of $E(0)$) is trivial for α sufficiently small. As $\alpha \rightarrow 0^+$ we obtain the thesis. \square

As a final remark, we note that for rectangular and polyrectangular initial sets the motion in case (1) coincides with the continuous crystalline motion described in [5].

References

- [1] R. Alicandro, A. Braides, and M. Cicalese. Phase and anti-phase boundaries in binary discrete systems: a variational viewpoint. *Netw. Heterog. Media* **1** (2006), 85–107
- [2] R. Alicandro and M. Cicalese, A general integral representation result for continuum limits of discrete energies with superlinear growth. *SIAM J. Math. Anal.* **36** (2004), 1–37.
- [3] R. Alicandro and M. Cicalese, Variational analysis of the asymptotics of the XY model. *Archive Ration. Mech. Anal.*, to appear.
- [4] R. Alicandro, M. Cicalese, and A. Gloria. Integral representation of the bulk limit of a general class of energies for bounded and unbounded spin systems. *Nonlinearity*, to appear
- [5] F. Almgren and J.E. Taylor. Flat flow is motion by crystalline curvature for curves with crystalline energies. *J. Differential Geom.* **42** (1995), 1-22.
- [6] F. Almgren, J.E. Taylor, and L. Wang. Curvature driven flows: a variational approach. *SIAM J. Control Optim.* **50** (1983), 387-438.
- [7] F.D. Arao Reis. Depinning transitions in interface growth models. *Brazilian J. Phys.* **33** (2003), 501-513
- [8] G. Bellettini, M. Novaga, M. Paolini, and C. Tornese, Convergence of discrete schemes for the Perona-Malik equation. Preprint Univ. di Pisa, 2006.
- [9] K. Bhattacharya and B. Craciun. Effective motion of a curvature-sensitive interface through a heterogeneous medium. *Interfaces Free Bound.* **6** (2004), 151-173
- [10] A. Braides. Handbook of Γ -convergence, in *Handbook of Differential Equations: Stationary PDEs, Volume 3* (M. Chipot, P. Quittner eds.), Elsevier, Amsterdam, 2006, 1-113.
- [11] A. Braides. *Approximation of Free-Discontinuity Problems*. Lecture Notes in Math. **1694**, Springer Verlag, Berlin, 1998.
- [12] A. Braides. *Γ -convergence for Beginners*. Oxford University Press, Oxford, 2002.

- [13] K. Brakke. *The Motion of a Surface by its Mean Curvature*. Mathematical Notes **20**. Princeton University Press, Princeton, N.J., 1978.
- [14] A. Carpio and L.L. Bonilla. Depinning transitions in discrete reaction-diffusion equations. *SIAM J. Appl. Math.* **63** (2003), 1056-1082.
- [15] N. Dirr and N. K. Yip. Pinning and de-pinning phenomena in front propagation in heterogeneous media. *Interfaces Free Bound.* **8** (2006), 79–109.
- [16] G. Fáth. Propagation failure of traveling waves in a discrete bistable medium. *Phys. D* **116** (1998), 176–190
- [17] M. Gage and R.S. Hamilton. The heat equation shrinking convex plane curves. *J. Differential Geom.* **23** (1986), 69–96.
- [18] K.B. Glasner. Homogenization of contact line dynamics. *Interfaces Free Bound.* **8** (2006), 523–542.
- [19] S.C. Glotzer, M.F. Gyure, F. Sciortino, A. Coniglio, and H.E. Stanley. Pinning in phase-separating systems. *Physical Review E* **49** (1994), 247-258
- [20] P.L. Lions and P.E. Souganidis. Homogenization of degenerate second-order PDE in periodic and almost-periodic environments and applications. *Ann. Inst. H. Poincaré Anal. Non Linéaire* **22** (2005), 667-677.
- [21] A. Prat and Y.-X. Li. Stability of front solutions in inhomogeneous media. *Phys. D* **186** (2003), 50-68
- [22] A. Stancu, Uniqueness of self-similar solutions for a crystalline flow, *Indiana Univ. Math. J.* **45** (1996), 1157-1174.
- [23] J. Xin and J. Zhu. Quenching and propagation of bistable reaction-diffusion fronts in multidimensional periodic media. *Phys. D* **81** (1995), 94-110.